Synthesis and properties of stabilized bis(2-oxo-2*H*-cyclohepta[*b*]-furan-3-yl)phenylmethyl and bis(1,2-dihydro-2-oxo-*N*-phenylcyclo-hepta[*b*]pyrrol-3-yl)phenylmethyl cations and their derivatives: remarkable substituent effect on the conformation and stability of the cations

Shin-ichi Naya and Makoto Nitta *

Department of Chemistry, School of Science and Engineering, and Materials Research Laboratory for Bioscience and Photonics, Waseda University, Shinjuku-ku, Tokyo 169-8555, Japan

Received (in Cambridge, UK) 17th August 2000, Accepted 11th September 2000
First published as an Advance Article on the web 8th November 2000

The reactions of benzaldehyde and 4-substituted benzaldehyde with 2*H*-cyclohepta[*b*]furan-2-one **5** and 1,2-dihydro-*N*-phenylcyclohepta[*b*]pyrrol-2-one **6** in TFA–CH_2Cl_2 afford two series of bis(2-oxo-2*H*-cyclohepta[*b*]furan-3-yl)arylmethanes **7a**–**e** and bis(1,2-dihydro-2-oxo-*N*-phenylcyclohepta[*b*]pyrrol-3-yl)arylmethanes **8a**–**e**, respectively. Upon oxidation reaction with DDQ followed by addition of 60% HPF_6, the methane derivatives **7a**–**e** and **8a**–**e** are converted to the corresponding methyl cations **9a**–**e**·PF_6^- and **10a**–**e**·PF_6^-, respectively. The stability of cations **9a**–**e** and **10a**–**e** is expressed by the pK_{R^+} values, which are determined spectrophotometrically, as 12.4 to 7.9 and 13.9 to 11.1, respectively. The electrochemical reductions of **9a**–**e** and **10a**–**e** exhibit reversible waves and low reduction potentials at −0.55 to −0.23 and −0.72 to −0.44 (V *vs.* Ag/Ag^+), respectively, upon cyclic voltammetry (CV); the values are lower than those of the related compounds, diazulen-1-ylarylmethyl cations. Good linear correlations between the pK_{R^+} values and $E1_{red}$ potentials of **9a**–**e** and **10a**–**e** are obtained. These values (pK_{R^+} and $E1_{red}$) are dependent on the substituents on the phenyl group; however, they do not correlate with the substituent constants of the Hammett equation. This feature is ascribed to the difference in the most stable conformation of the three aromatic groups in the cations; the phenyl group having a more electron-donating substituent is prone to become more planar to the reference plane. The most stable conformation is deduced on the basis of MO calculations (MOPAC, AM1 method). The ^{1}H NMR and UV–vis spectral studies also rationalize the conformational change of the three aromatic rings, depending on the substituent on the benzene ring. On the basis of the study, the stabilizing ability of the 4-substituted phenyl group and heteroazulenes for the cations is clarified to be in the order of 4-dimethylaminophenyl > 1,2-dihydro-2-oxo-*N*-phenylcyclohepta[*b*]pyrrol-3-yl > 2-oxo-2*H*-cyclohepta-[*b*]furan-3-yl ~ 4-methoxyphenyl.

Introduction

Recently, the synthesis and properties of a series of extremely stabilized azulene analogues of the triphenylmethyl cation, *i.e.*, triazulen-1-ylmethyl,[1–7] diazulen-1-ylphenylmethyl,[1,4,6–10] and azulen-1-yldiphenylmethyl cations[1,4,6,7,9] and their derivatives, have been investigated extensively. Regarding the azulene-substituted methyl cations, theoretical calculations and a large dipole moment of azulene reasonably predict that azulene should stabilize carbocations attached at the 1-position to exhibit good stability with high pK_{R^+} values. Since heteroazulenes such as 2*H*-cyclohepta[*b*]furan-2-one **5**[11] and 1,2-dihydro-*N*-phenylcyclohepta[*b*]pyrrol-2-one **6**[12] (Scheme 1) have a molecular framework similar to that of azulene and undergo electrophilic attack at the 3-position,[13,14] thus, the heteroazulenes **5** and **6** should also stabilize cations attached at the 3-position. From this point of view, we have recently reported the synthesis and properties of heteroazulene analogues of the triphenylmethyl cations, tris(2-oxo-2*H*-cyclohepta[*b*]furan-3-yl)-, tris(1,2-dihydro-2-oxo-*N*-phenyl-cyclohepta[*b*]pyrrol-3-yl)-, and tris(1,2-dihydro-*N*-methyl-2-oxocyclohepta[*b*]pyrrol-3-yl)methyl cations, **1a**–**c**.[15] The proton signals in the ^{1}H NMR spectra of **1a**–**c** appeared as broad signals, and this feature is ascribed to the slow conformational change arising from steric hindrance of three bulky heteroazulenes. The pK_{R^+} values of these cations **1a**–**c** were measured to be 9.7, 12.2, and 13.1, respectively, and the reduction potentials were also measured to characterize the properties of the cations. The pK_{R^+} values of **1a**–**c** are 16.1–19.5 pH units higher than the value of the triphenylmethyl cation (pK_{R^+} = −6.44)[16] and are close to the values of the triazulen-1-ylmethyl cation (pK_{R^+} = 10.5) and its derivatives. The reduction potentials of **1a**–**c** were −0.31 to −0.62 ($E1_{red}$) and −0.95 to −1.33 ($E2_{red}$), and two reduction waves were reversible. These values are much lower than those of the triazulen-1-ylmethyl cation derivatives, and thus, heteroazulenes are shown to stabilize not only cations, but also the corresponding radicals and anions. The energy levels of the LUMO obtained by MO calculation (MOPAC, AM1 method)[17] of azulene, **5** and **6** are −0.87, −1.19, and −0.93 eV, and the energy levels of the HOMO are calculated to be −8.02, −8.69, and −8.28 eV, respectively. The stabilizing effect of **5** and **6** toward the radical and anion species would be ascribed to the low-lying HOMO and/or LUMO. On the other hand, the synthesis and properties of Malachite Green (4,4′-bis(dimethylamino)triphenylmethyl chloride) derivatives **2a**–**d**[18] and diazulen-1-yl(4-substituted-phenyl)methyl cation derivatives **3a**–**c**,[4,6,9] have been investigated to gain insight into the substituent effect. The pK_{R^+} values of these cations depend on the substituents on the phenyl group. The pK_{R^+} values of **2a**–**c**[18] were determined to be 9.36, 7.18, and 6.84, respectively,

DOI: 10.1039/b006752k

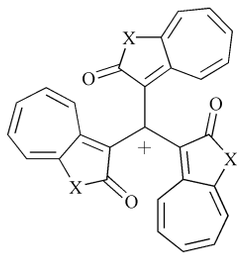

1a : X = O
b : X = NPh
c : X = NMe

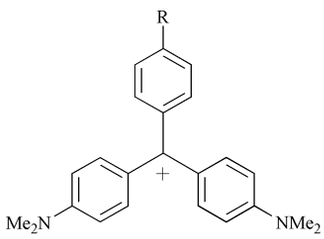

2a-d
a: R = NMe_2
b: R = OMe
c: R = H
d: R = Cl

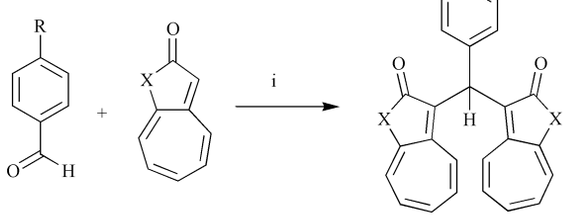

4a-e **5** : X = O; **6** : X = NPh **7a-e** : X = O; **8a-e** : X = NPh

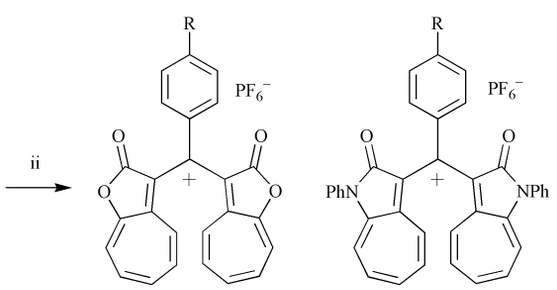

9a-e•PF_6^- **10a-e•PF_6^-**

a : R = NMe_2; **b**: R = OMe; **c** : R = H; **d** : R = Cl; **e** : R = CN

Scheme 1 *Reagents and conditions*: i, CH_2Cl_2–TFA (5:1), rt; ii, (a) DDQ in CH_2Cl_2; (b) 60% HPF_6.

and those of **3a**–**c**[4,6,9] were also measured to be 13.2, 11.7, and 10.7, respectively. In order to clarify the stabilizing effect of heteroazulenes in cations, related radicals and anion species, we studied the synthesis and properties of bis(2-oxo-2*H*-cyclohepta[*b*]furan-3-yl)-, bis(1,2-dihydro-2-oxo-*N*-phenyl-

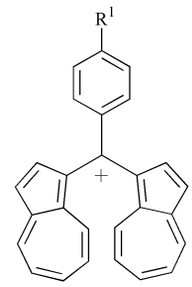

3a-c
a : R^1 = NMe_2
b : R^1 = OMe
c : R^1 = H

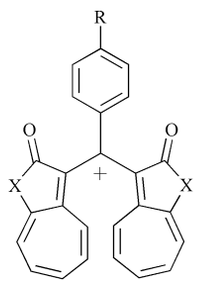

9a-e : X = O **10a-e** : X = NPh
a : R = NMe_2; **b**: R = OMe
c : R = H; **d** : R = Cl
e : R = CN

cyclohepta[*b*]pyrrol-3-yl)phenylmethyl cations, and their 4-substituted phenyl derivatives, **9a**–**e** and **10a**–**e**. From the substituent effect on **9a**–**e** and **10a**–**e**, a linear free energy relationship between the $E1_{red}$ and pK_{R^+} is obtained. Moreover, comparisons of the stabilizing effect of heteroazulenes **5** and **6** with that of the 4-substituted phenyl group were investigated. The most stable conformations of **9a**–**e** and **10a**–**e** are predicted on the basis of MO calculations (MOPAC, AM1 method).[17] The deviations of the three aromatic groups of **9a**–**e** and **10a**–**e** depend on the electron-donating ability of the 4-substituted phenyl group. The ^1H NMR and UV–vis spectral studies rationalize the difference in conformation of the three aromatic groups of cations **9a**–**e** and **10a**–**e**. We report herein the results in detail.

Results and discussion

Synthesis

Although substituted benzaldehydes had reacted with azulenes in acetic acid to give diazulen-1-ylarylmethane derivatives,[1–10] the heteroazulene **5** did not react with 4-dimethylaminobenzaldehyde in acetic acid at room temperature for 96 h, and **5** was recovered quantitatively. Thus, the condensation reactions of heteroazulenes **5** and **6** with benzaldehyde and 4-substituted benzaldehydes **4a**–**e** were carried out in CH_2Cl_2–TFA (5:1) to give the methane derivatives **7a**–**e** and **8a**–**e** in good yield, respectively (Scheme 1, Table 1).[15] The structures of the methane derivatives **7a**–**e** and **8a**–**e** were assigned on the basis of their IR, ^1H and ^{13}C NMR spectral data, as well as mass spectral data and elemental analyses. The hydride abstractions of **7a**–**e** and **8a**–**e** with DDQ in CH_2Cl_2 at room temperature followed by addition of 60% aqueous HPF_6 solution gave the salts **9a**–**e**·PF_6^- and **10a**–**e**·PF_6^- in the yields listed in Table 1.

Spectroscopic properties of 9a–e·PF_6^- and 10a–e·PF_6^-

The salts **9a**–**e**·PF_6^- and **10a**–**e**·PF_6^- crystallized easily to give

Table 1 Results for the preparation of methane derivatives **7a–e** and **8a–e**, and methylium salts **9a–e·PF_6^-** and **10a–e·PF_6^-**

		Condensation		Hydride abstraction	
Benzaldehyde **4a–e**	Compound **5** or **6**	Product	Yield (%)	Product	Yield (%)
4a	**5**	**7a**	100	**9a·PF_6^-**	100
4b	**5**	**7b**	97	**9b·PF_6^-**	98
4c	**5**	**7c**	93	**9c·PF_6^-**	100
4d	**5**	**7d**	96	**9d·PF_6^-**	81
4e	**5**	**7e**	100	**9e·PF_6^-**	71
4a	**6**	**8a**	100	**10a·PF_6^-**	100
4b	**6**	**8b**	81	**10b·PF_6^-**	100
4c	**6**	**8c**	88	**10c·PF_6^-**	85
4d	**6**	**8d**	74	**10d·PF_6^-**	80
4e	**6**	**8e**	71	**10e·PF_6^-**	62

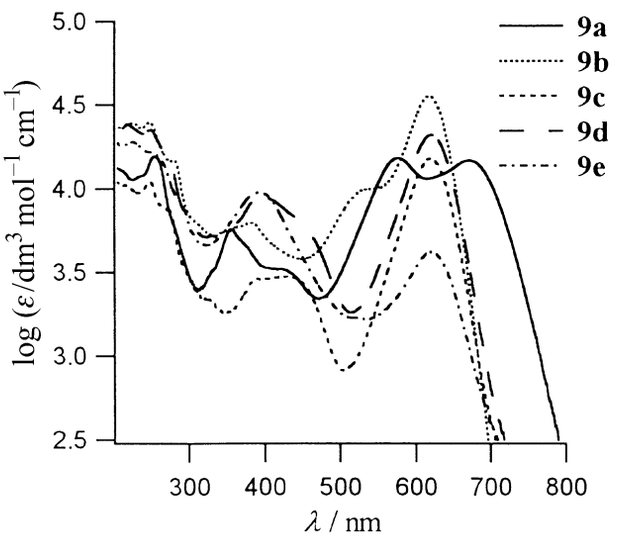

Fig. 1 UV–vis spectra of cations **9a–e** in acetonitrile.

complexes containing H_2O or a solvent or HPF_6 in the crystal lattice; this feature is similar to the cases of triheteroazulen-3-ylmethyl cations **1a–c** and Crystal Violet [tris(4-dimethylaminophenyl)methyl chloride], which forms two crystal structures containing H_2O as the monohydrate and the nonahydrate.[19] Thus, satisfactory analytical data of these salts were not obtained; however, mass spectra of **9a–e·PF_6^-** and **10a–e·PF_6^-** ionized by FAB exhibited the correct M^+–PF_6 ion peaks, which are indicative of the cationic structure of these compounds. The characteristic absorption bands of the counter ion PF_6^- are observed at 838–845 cm^{-1} in the IR spectra of **9a–e·PF_6^-** and **10a–e·PF_6^-**. UV–vis spectra of **9a–e** and **10a–e** in CH_3CN are shown in Fig. 1 and 2, respectively. The spectra of **9b–e** and **10b–e** resemble each other, while the spectra of **9a** and **10a**, both of which have a dimethylamino group, show remarkable changes and an appreciable red-shift by 50 and 25 nm in the longest wavelength absorption maxima, as compared with those of the other cations, respectively (*vide infra*). In the ^1H NMR spectra, the methine protons (δ 5.23–6.28) of methane derivatives **7a–e** and **8a–e** disappeared in the salts **9a–e·PF_6^-** and **10a–e·PF_6^-**. Although the proton signals of **9a–e·PF_6^-** appear as sharp signals, the proton signals on the seven-membered ring of **10a–e·PF_6^-** appear as several broad signals. Thus, the slow conformational change of the heteroazulene moieties of **10a–e·PF_6^-** would occur on the ^1H NMR time scale at room temperature, probably because of the steric hindrance. The two heteroazulene rings in each of **9a–e·PF_6^-** and **10a–e·PF_6^-** are observed to be equivalent in the ^1H NMR spectra. These characteristics are also observed in the ^{13}C NMR spectra of **9a–e·PF_6^-** and **10a–e·PF_6^-**.

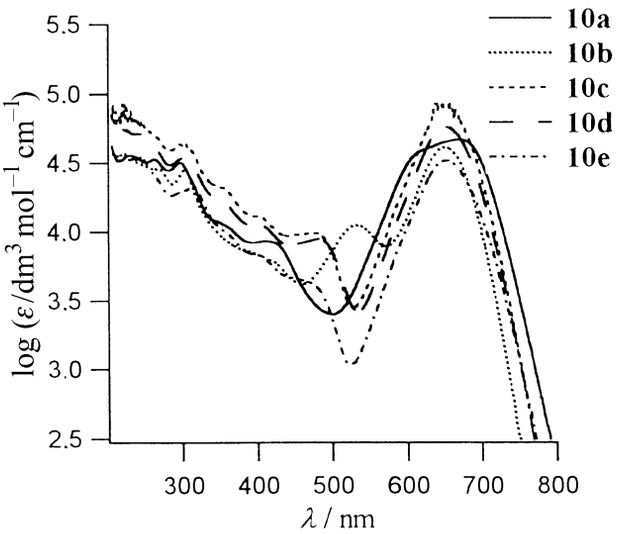

Fig. 2 UV–vis spectra of cations **10a–e** in acetonitrile.

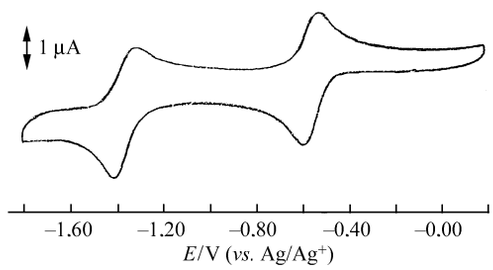

Fig. 3 Cyclic voltammogram of **10c** in MeCN.

Stability of the methyl cations 9a–e and 10a–e: pK_{R^+} values and reduction potentials ($E1_{red}$ and $E2_{red}$)

The affinity of the carbocation toward hydroxide ions, expressed by the pK_{R^+} value, is the most common criterion of carbocation stability.[20] The pK_{R^+} values of the cations **9a–e** and **10a–e** are obtained spectrophotometrically and summarized in Table 2 along with those of the reference compounds diazulen-1-ylphenylmethyl cations **3a–c**.[4,6,9] The equilibrium of the reaction of the hydroxide ion with **9a–e** and **10a–e** is not completely reversible. This feature may be ascribed to the instability of neutralized products under the conditions of the pK_{R^+} measurement. Immediate (5 s) acidification of alkaline solutions (*ca.* pH 14) of **9a–e** and **10a–e** with TFA regenerated the absorption maxima of the cations in the visible regions in 85–90%. As expected, the heteroazulenes **5** and **6** effectively stabilize the cations, and the pK_{R^+} values of **9a–e** and **10a–e** are extremely high, as in the cases of triheteroazulen-3-ylmethyl cations **1a–c**.[15] The pK_{R^+} values of the cations **9a–c** are slightly lower by 0.8–1.5 pH units than those of the diazulen-1-ylphenylmethyl cations **3a–c** having a similar substituent on the 4-position of the phenyl group, respectively,[4,6,9] while the cations **10a–c** express higher pK_{R^+} values by 0.7–1.5 pH units than those of the cations **3a–c**, respectively (Table 2). The cations **10a–e** are more stable than **9a–e**, respectively, because of the electron-donating property of the nitrogen atom.

The reduction potentials of **9a–e** and **10a–e** determined by cyclic voltammentry (CV) in CH_3CN are also summarized in Table 2, together with those of the reference cations **3a–c**.[4,6,9] The reduction waves of **9a–e** and **10a–e** were reversible under the conditions of CV measurements, and they showed two reversible waves (Fig. 3 for **10c** and Table 2). The two waves were explained by the formation of stable radical species **11a–e** and **12a–e** and anion species **13a–e** and **14a–e**, respectively (Scheme 2). These reduction behaviors of **9a–e** and **10a–e** are similar to those of cations **1a–c**.[15] Consequently, the

Table 2 pK_{R^+} values and reduction potentials[a] of cations **9a–e**,[b] **10a–e**[b] and reference compounds **3a–c**

Compound	pK_{R^+}	$E1_{red}$	($E_{cathode}$, E_{anode})	$E2_{red}$	($E_{cathode}$, E_{anode})
9a	12.4	−0.55	(−0.58, −0.51)	−1.15	(−1.20, −1.09)
9b	10.0	−0.36	(−0.40, −0.33)	−1.08	(−1.13, −1.02)
9c	9.3	−0.31	(−0.34, −0.28)	−1.03	(−1.08, −0.99)
9d	9.1	−0.29	(−0.32, −0.26)	−0.99	(−1.03, −0.94)
9e	7.9	−0.23	(−0.26, −0.20)	−0.88	(−0.90, −0.86)
10a	13.9	−0.71	(−0.74, −0.68)	−1.37	(−1.43, −1.31)
10b	12.2	−0.58	(−0.60, −0.55)	−1.31	(−1.36, −1.26)
10c	12.0	−0.53	(−0.56, −0.50)	−1.29	(−1.32, −1.25)
10d	12.0	−0.51	(−0.54, −0.48)	−1.26	(−1.30, −1.22)
10e	11.1	−0.44	(−0.47, −0.41)	−1.08	(−1.10, −1.38)
3a[c]	13.2	−0.87		−1.64[f]	
3b[d]	11.7	−0.71		−1.55[f]	
3c[e]	10.5	−0.66		−1.52[f]	

[a] V *vs.* Ag/Ag^+; mean value of the cathodic and anodic peaks. [b] **9a–e**·PF_6^- and **10a–e**·PF_6^- were used for the measurement. [c] Ref. 9. [d] Ref. 6. [e] Ref. 4. [f] Irreversible process.

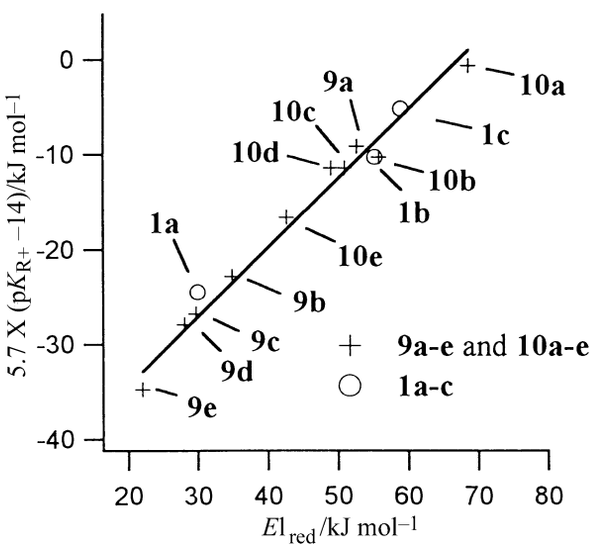

Fig. 4 Plot of pK_{R^+} values against $E1_{red}$ of **9a–e**, **10a–e**, and **1a–c**.

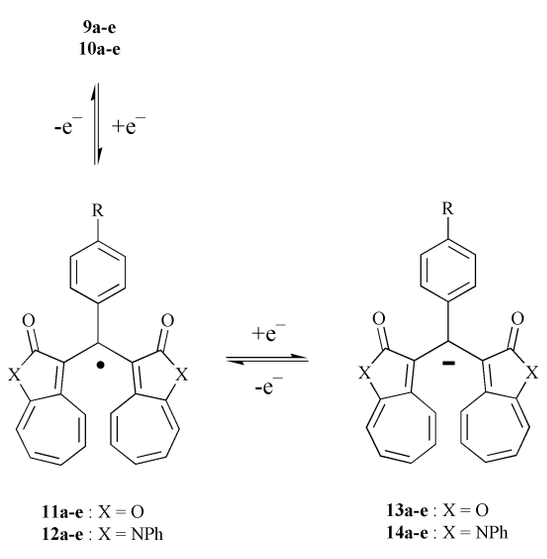

Scheme 2

heteroazulene rings stabilize not only carbocations, but also radical species **11a–e** and **12a–e** and anions **13a–e** and **14a–e**. The stabilizing effect of heteroazulenes toward the radical species would be attributable to the captodative effect[21] of the electron-withdrawing carbonyl group and the electron-donating oxygen and nitrogen atoms in the heteroazulene moieties.

In Fig. 4, pK_{R^+} values of cations **9a–e** and **10a–e** were plotted against $E1_{red}$ of these cations. The units of $E1_{red}$ and pK_{R^+} values were converted to kJ mol^{-1} [−96.5 kJ mol^{-1} × $E1_{red}$/V and 5.7 kJ mol^{-1} × (pK_{R^+} − 14)]. A linear correlation line was obtained, and the slope and *y*-intercept of this line were 0.72 and −48.35, respectively (eqn. (1), correlation coefficient = 0.991).

$$(\Delta G_i) = 0.72\ (\Delta G_{et}) - 48.35 \quad (1)$$

Okamoto *et al.* have reported the linear free energy relationships of substituted tropyl and cyclopropenyl cations.[22] By a modified analysis, the reaction of the cation with the hydroxide ion (eqn. (2)) is divided into an electron-transfer reaction (eqn. (3)) and a radical-coupling reaction (eqn. (4)). The free-

$$\begin{cases} R^+ + {}^-OH \rightleftharpoons ROH \quad \Delta G_i & (2) \\ R^+ + e^- \rightleftharpoons R^\bullet \quad \Delta G_{et} & (3) \\ R^\bullet + {}^\bullet OH \rightleftharpoons ROH \quad \Delta G_d & (4) \end{cases}$$

energy difference for the reaction of the cation with the hydroxide ion (ΔG_i in eqn. (2)) is derived from the pK_{R^+} values, and the free-energy difference of the electron-transfer reaction (ΔG_{et} in eqn. (3)) is derived from the first reduction potential ($E1_{red}$). According to this definition, the more stable cation has larger ΔG_i and ΔG_{et} values. However, the ΔG_{et} represents the difference in thermodynamic stability between the cations and the corresponding radicals. Eqn. (5), (6) and (7) are obtained by the

$$\begin{cases} R_1OH + R_2^+ \rightleftharpoons R_1^+ + R_2OH \quad \Delta\Delta G_i & (5) \\ R_1^\bullet + R_2^+ \rightleftharpoons R_1^+ + R_2^\bullet \quad \Delta\Delta G_{et} & (6) \\ R_1OH + R_2^\bullet \rightleftharpoons R_1^\bullet + R_2OH \quad \Delta\Delta G_d & (7) \end{cases}$$

subtraction of eqn. (2), (3) and (4) for one cation from those for the other cation, and thus, they show the difference in stability for the two cations. By this definition, $\Delta\Delta G_i$ represents the sum of $\Delta\Delta G_{et}$ and $\Delta\Delta G_d$ (eqn. (8)), and the value of $\Delta\Delta G_i$ divided by $\Delta\Delta G_{et}$ corresponds to the slope of the regression line (eqn. (9)). The slope of the line was obtained as 0.72, which is smaller than 1.0. Hence, from eqn. (8) and (9), $\Delta\Delta G_d$ linearly

$$\Delta\Delta G_i = \Delta\Delta G_{et} + \Delta\Delta G_d \quad (8)$$

$$\Delta\Delta G_i = 0.72\ \Delta\Delta G_{et} \quad (9)$$

correlates with $\Delta\Delta G_{et}$ with a negative slope (−0.28), eqn. (10).

Table 3 Hammett substituent constants σ_p[a] and dihedral angles θ_1–θ_3 for the most stable conformation of cations **9a**–**e** and **10a**–**e**

Compound	R	σ_p[a]	θ_1[b]/ deg	θ_2[b]/ deg	θ_3[b]/ deg
9a	NMe_2	−0.83	39.5	16.9	40.2
9b	OMe	−0.27	41.7	17.4	39.3
9c	H	0	59.1	18.7	30.9
9d	Cl	0.23	58.3	18.9	31.3
9e	CN	0.66	59.6	18.5	31.2
10a	NMe_2	−0.83	42.1	18.2	44.7
10b	OMe	−0.27	49.2	16.1	43.0
10c	H	0	59.5	16.7	40.5
10d	Cl	0.23	59.2	16.6	40.3
10e	CN	0.66	62.0	16.6	39.5

[a] Ref. 24. [b] Dihedral angles θ_1–θ_3 (in deg) denote deviation of the planes of the heteroazulenes and phenyl group from the reference plane (Fig. 6).

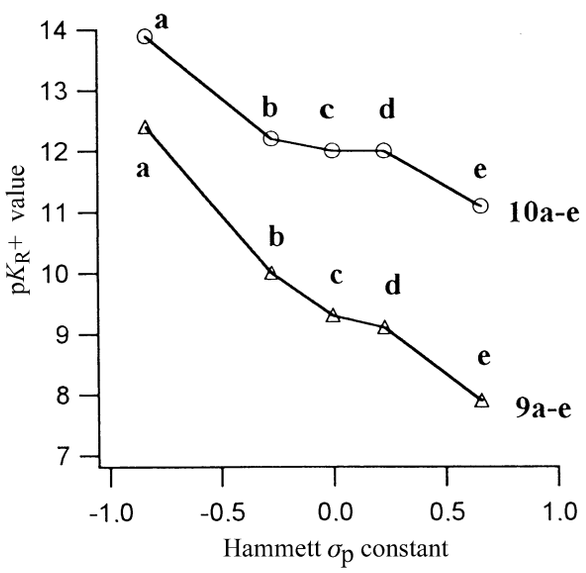

Fig. 5 The Hammett plot of pK_{R^+} values of **9a**–**e** and **10a**–**e**.

$$\Delta\Delta G_d = -0.28\ \Delta\Delta G_{et} \quad (10)$$

Therefore, from eqn. (10) it can be deduced that the more stable cation gives a less stable radical in single-electron reduction of **9a**–**e** and **10a**–**e**. Thus, the more electron-donating substituent on the phenyl group not only stabilizes the cations, but also destabilizes the radicals. The plots of the cation **1a**–**c** lie on the same regression line. This feature suggests that cations **9a**–**e**, **10a**–**e**, and **1a**–**c** are stabilized in a similar manner.

Substituent effect and conformational change for cations 9a–e and 10a–e

The correlation between the pK_{R^+} values of **9a**–**e** and **10a**–**e** and Hammett constants σ_p[23] of the substituent on the phenyl group is shown in Fig. 5. No linear correlations are obtained; the pK_{R^+} values are larger than the expected values when the electron-withdrawing substituents are introduced on the phenyl group. In order to gain insight into the relationship, MO calculations of the cations **9a**–**e** and **10a**–**e** were carried out using the AM1 method (MOPAC97).[17] A larger π-conjugative effect is obtained with a more planar conformation, while the more planar conformation experiences larger steric hindrance between the substituted aromatic rings. The most stable conformations of **9a**–**e** and **10a**–**e** obtained by MO calculations are summarized in Table 3. The dihedral angles, θ_1, θ_2, and θ_3, express deviation from the plane of the phenyl group and heteroazulenes from the reference plane (the plane which is defined by the three arylic *ipso* carbons, Fig. 6). In Fig. 7 and 8,

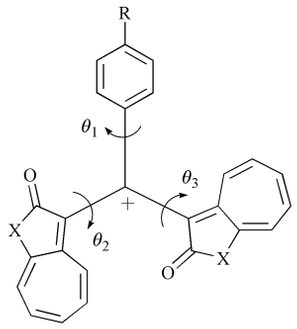

7a-e: X = O
8a-e: X = NPh
a : R = NMe_2; **b**: R = OMe; **c** : R = H
d : R = Cl; **e** : R = CN

Fig. 6

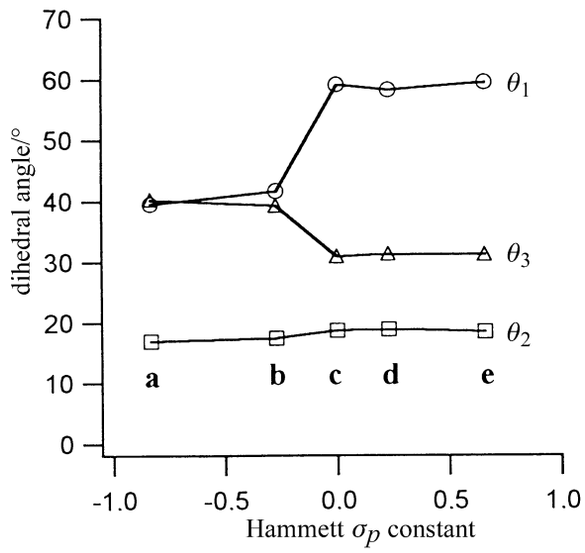

Fig. 7 The Hammett plot of dihedral angles of **9a**–**e**.

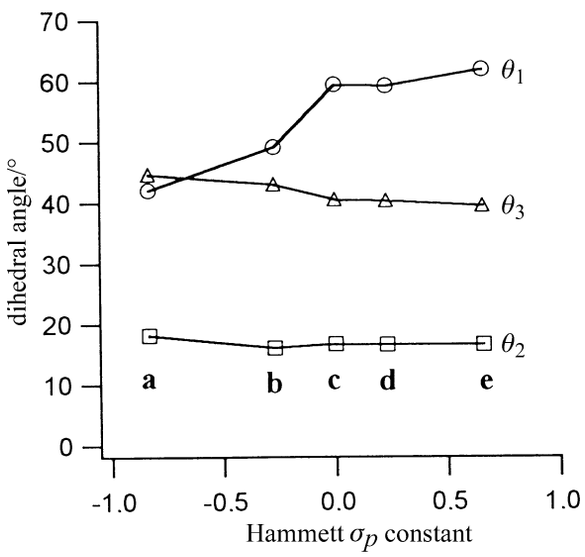

Fig. 8 The Hammett plot of dihedral angles of **10a**–**e**.

the θ_1, θ_2, and θ_3 values of **9a**–**e** and **10a**–**e** were plotted against the substituent constants of the Hammett equation. Since the ^{1}H NMR spectra of **9a**–**e** and **10a**–**e** show two heteroazulene moieties to be equivalent, the heteroazulene rings of these cations can rotate freely around the most stable conformations. The dihedral angle of one of the heteroazulenes (θ_2) does not depend on the substituent on the phenyl group. However, the

Table 4 The longest wavelength absorption maxima in UV–vis spectra of cations **9a**–**e**, **10a**–**e**, **2a**–**d**, and **3a**–**c**

		$\lambda_{max}(CH_3CN)$/nm			
	R	**9a**–**e**	**10a**–**e**	**2a**–**d** [a]	**3a**–**c**
a	NMe_2	671 575	677 614 [b]	592	615 [c]
b	OMe	621	652	615	626 [d]
c	H	621	652	623	639 [e]
d	Cl	621	652	627	—
e	CN	621	652	—	—

[a] Ref. 18. [b] Shoulder. [c] Ref. 9. [d] Ref. 6. [e] Ref. 4.

decrease of electron-donating ability of the substituent induces an increase of θ_1 and decrease of θ_3. These features may be explained as follows: the phenyl group having large electron-donating ability becomes more planar with the reference plane (small dihedral angle θ_1) to stabilize the cation effectively. If the electron-donating ability of the substituent on the phenyl group were decreased, heteroazulenes become planar with the reference plane to stabilize the cations, and thus, the cations do not lose stability as expected by the Hammett equation.

This nature is confirmed by ^{1}H NMR and UV–vis spectral data. Five proton signals on the seven-membered ring of the heteroazulene of the cations **9a**–**e** are shifted to low-field compared with those of methanes **7a**–**e**. The differences between the average chemical shifts ($\Delta\delta_{av}$) on the seven-membered ring of the cations **9a**–**e** and those of methanes **7a**–**e** are 0.68, 1.03, 1.05, 1.06, and 1.04 ppm, respectively. Since the difference between **9a** and **7a** is smaller than that of the other cations **9b**–**e**, the positive charge is more delocalized on the phenyl group for **9a** as compared with those of the other cations **9b**–**e**. In contrast, the positive charge is more delocalized on the heteroazulene moiety for cations **9b**–**e**. A similar tendency is observed for cations **10a**–**e**, and the differences ($\Delta\delta_{av}$) between **10a**–**e** and **8a**–**e** are 0.47, 0.75, 0.78, 0.78, and 0.78 ppm, respectively. Thus, the plane of the phenyl group is more planar to the reference plane for cations **9a** and **10a** while, for cations **9b**–**e** and **10b**–**e**, the plane of the phenyl group is less planar to the reference plane.

The UV–vis spectra of **9a**–**e** and **10a**–**e** also suggest a change of conformation (deviation of the planes of the heteroazulenes and phenyl group). The longest wavelength absorption maxima of **9a**–**e** and **10a**–**e** are given in Table 4, along with those of **2a**–**d** and **3a**–**c**. The longest wavelength absorption maxima of **2a**–**d** appear at 592 to 627 nm,[18] and those of **3a**–**c** appear at 615 to 639 nm.[4,6,9] The decrease of electron-donating ability of the substituent on the phenyl group induces a red shift of the maxima. This behavior has been explained by MO calculations.[24] Since the decrease of electron-donating ability of the substituent on a position having a large coefficient in the LUMO causes lowering of the energy level in the LUMO, this change causes a red shift of the absorption maxima (*i.e.*, **2a**–**d**, **3a**–**c**). In a similar manner, the decrease of electron-donating ability of the substituent on a position having a large coefficient in the HOMO induces lowering of the energy level in the HOMO, and thus, causes the blue shift of the absorption maxima. However, no change in the absorption maxima of **9b**–**e** and **10b**–**e** is observed. These features are explained as follows: since the plane of the phenyl group in **9b**–**e** and **10b**–**e** is twisted against the reference plane (large θ_1), the phenyl groups in **9b**–**e** and **10b**–**e** do not have effective π-conjugation to the cationic center (*vide supra*). Thus, the 4-position of the phenyl group in **9b**–**e** and **10b**–**e** has no coefficient in the HOMO or LUMO. In contrast, the absorption maxima of **9a** and **10a** appear as two bands and are different from those of **9b**–**e** and **10b**–**e**. The additional band may arise from the contribution of the canonical structure of dimethyl(4-methylidenecyclohexa-2,5-dien-1-ylidene)ammonium for the 4-dimethylaminophenyl group. This feature is also a typical property of triphenylmethyl cation derivatives. Thus, the plane of the phenyl group having greater stabilizing ability on **9a** and **10a** is more planar with respect to the reference plane, and **9a** and **10a** have two absorption maxima like the triphenylmethyl cation derivatives. Thus, the UV–vis spectra can also rationalize the conformational change of the three aromatic rings, depending on the substituent on the phenyl group. Based on the present studies, the stabilizing ability of the 4-substituted phenyl group and heteroazulenes on the cations is found to be in the order of 4-dimethylaminophenyl > 1,2-dihydro-2-oxo-*N*-phenylcyclohepta[*b*]-pyrrol-3-yl > 2-oxo-2*H*-cyclohepta[*b*]furan-3-yl ~ 4-methoxyphenyl.

Conclusion

Efficient synthesis and properties of relatively stable novel types of diheteroazulen-3-ylphenylmethyl cations **9a**–**e** and **10a**–**e** have been studied. The stabilities of **9a**–**e** and **10a**–**e** were examined by the pK_{R^+} values and the reduction potentials were measured by CV. A good linear correlation between pK_{R^+} values and reduction potentials was obtained for the cations **9a**–**e** and **10a**–**e** and the heteroazulenes are found to stabilize not only cations but also radicals and anions. The pK_{R^+} values of the cations **9a**–**e** and **10a**–**e** did not correlate with the substituent constants of the Hammett equation. This was ascribed to the conformational change depending on the electron-donating ability of the 4-substituted phenyl group.

Experimental

IR spectra were recorded on a HORIBA FT-710 spectrometer. Mass spectra and high-resolution mass spectra were run on JMS-AUTOMASS 150 and JMS-SX102A spectrometers. Unless otherwise specified, ^{1}H NMR spectra and ^{13}C NMR spectra were recorded on a JNM-lambda 500 spectrometer using $CDCl_3$ as the solvent, and the chemical shifts are given relative to $SiMe_4$ as internal standard: *J*-values are given in Hz. Mps were recorded on a Yamato MP-21 apparatus and are uncorrected. The heteroazulenes, 2*H*-cyclohepta[*b*]furan-2-one **5**[11] and 1,2-dihydro-*N*-phenylcyclohepta[*b*]pyrrol-2-one **6**[12] were prepared as described previously.

General procedure for the preparation of heteroazulene-substituted methanes 7a–e and 8a–e

A solution of heteroazulene **5** (2 mmol) or **6** (2 mmol) and benzaldehyde or 4-substituted benzaldehyde **4** (1 mmol) in a mixture of CH_2Cl_2 (10 cm^3) and TFA (2 cm^3) was stirred at rt for 24 h. After the reaction was completed, the reaction mixture was poured into aqueous $NaHCO_3$ solution. The mixture was extracted with CH_2Cl_2, and the extract was dried over Na_2SO_4 and concentrated *in vacuo*. The resulting residue was purified through column chromatography on Al_2O_3 by using hexane–ethyl acetate (1 : 1) as the eluent to give the products **7a**–**e** and **8a**–**e**. The results are summarized in Table 2.

Compound 7a. Orange prisms; mp 216–217 °C (from EtOH); δ_H (500 MHz) 2.93 (6H, s, Me), 5.60 (1H, s, CH), 6.69 (2H, d, *J* 8.8, Ph-3,5), 6.75–6.79 (2H, m, H-6), 6.91–6.95 (6H, m, H-5,7,8), 7.07 (2H, d, *J* 8.8, Ph-2,6), 7.43 (2H, d, *J* 11.4, H-4); δ_C (125.7 MHz) 34.4, 40.6, 109.7, 112.9, 113.7, 124.4, 128.2, 128.3, 130.8, 131.9, 134.4, 148.5, 149.5, 157.6, 169.6; $\nu_{max}(CCl_4)$/cm^{-1} 1757, 1267; *m*/*z* (rel. int.) 423 (M^+, 68.5), 234 (100%) (Found: C, 76.6; H, 4.9; N, 3.3. $C_{27}H_{21}NO_4$ requires C,76.58; H, 5.00; N, 3.31%).

Compound 7b. Orange needles; mp 137–139 °C (from AcOEt); δ_H (500 MHz) 3.80 (3H, s, Me), 5.64 (1H, s, CH), 6.76–6.82 (2H, m), 6.86 (2H, d, *J* 8.8, Ph-2, 6), 6.93–6.98 (6H, m),

7.13 (2H, d, *J* 8.8, Ph-3,5), 7.44 (2H, d, *J* 11.4, H-4); δ_C (125.7 MHz) 34.4, 55.3, 109.2, 114.0, 114.2, 128.2, 128.6, 130.4, 131.0, 132.1, 134.6, 148.6, 157.6, 158.5, 169.5; $\nu_{max}(CHCl_3)/cm^{-1}$ 1743, 1271; *m/z* (rel. int.) 410 (M^+, 100%) (Found: C, 74.3; H, 4.4. $C_{26}H_{18}O_5 \cdot \frac{1}{2}H_2O$ requires C, 74.45; H, 4.57%).

Compound 7c. Orange powder; mp 225–225 °C (from CH_2Cl_2–EtOH); δ_H (500 MHz) 5.70 (1H, s, CH), 6.77–6.83 (2H, m), 6.94–6.99 (6H, m), 7.23 (2H, d, *J* 8.1, Ph-2,6), 7.27 (1H, t, *J* 7.7, Ph-4), 7.33 (2H, dd, *J* 8.1, 7.7, Ph-3,5), 7.43 (2H, d, *J* 11.3, H-4); δ_C (125.7 MHz) 35.0, 108.9, 114.1, 127.0, 127.6, 128.2, 128.8, 131.0, 132.2, 134.6, 136.9, 148.6, 157.6, 169.5; $\nu_{max}(CHCl_3)/cm^{-1}$ 1743, 1271; *m/z* (rel. int.) 380 (M^+, 88.1), 77 (100%) (Found: C, 78.8; H, 4.0. $C_{25}H_{16}O_4$ requires C, 78.94; H, 4.24%).

Compound 7d. Orange prisms; mp 204–205 °C (from CH_2Cl_2–EtOH); δ_H (500 MHz) 5.66 (1H, s, CH), 6.80–6.86 (2H, m), 6.96–7.03 (6H, m), 7.16 (2H, d, *J* 8.6, Ph-3,5), 7.29 (2H, d, *J* 8.6, Ph-2,6), 7.48 (2H, d, *J* 11.6, H-4); δ_C (125.7 MHz) 34.5, 108.4, 114.3, 128.1, 128.9, 129.0, 131.1, 132.4, 132.8, 135.0, 148.7, 157.6, 169.4; $\nu_{max}(CHCl_3)/cm^{-1}$ 1743, 1267; *m/z* (rel. int.) 414 (M^+, 100%), 416 (33.4) (Found: C, 72.1; H, 3.4. $C_{25}H_{15}ClO_4$ requires C, 72.38; H, 3.64%).

Compound 7e. Yellow powder; mp 155–156 °C (from CH_2Cl_2–EtOH); δ_H (500 MHz) 5.23 (1H, s, CH), 6.86–6.91 (2H, m, H-6), 7.01–7.08 (6H, m, H-5,7,8), 7.35 (2H, d, *J* 8.5, Ph-2,6), 7.51 (4H, d, *J* 11.6, H-4), 7.63 (2H, d, *J* 8.5, Ph-3,5); δ_C (125.7 MHz) 35.0, 107.6, 110.9, 114.8, 118.7, 127.9, 128.4, 131.4, 132.5, 132.7, 135.4, 142.5, 148.9, 157.6, 169.2; ν_{max}(KBr)/cm^{-1} 2225, 1740, 1271; *m/z* (rel. int.) 405 (M^+, 99.0), 232 (100%) (Found: C, 76.0; H, 3.7; N, 3.3. $C_{25}H_{15}NO_4 \cdot \frac{1}{4}H_2O$ requires C, 76.18; H, 3.81; N, 3.42%).

Compound 8a. Orange powder; mp 265–266 °C (from CH_2Cl_2–EtOH); δ_H (500 MHz) 2.92 (6H, s, Me), 6.16 (1H, s, CH), 6.71–6.76 (6H, m, H-6,8, Ph-2,6), 6.83 (2H, dd, *J* 10.2, 9.6, H-7), 6.89 (2H, dd, *J* 11.4, 8.5, H-5), 7.23 (2H, d, *J* 8.7, Ph-3,5), 7.35 (4H, d, *J* 8.5, NPh-2,6), 7.41 (2H, t, *J* 7.3, NPh-4), 7.50 (4H, dd, *J* 8.5, 7.3, NPh-3,5), 7.84 (2H, d, *J* 11.4, H-4); δ_C (125.7 MHz) 35.2, 40.9, 112.7, 113.1, 114.2, 127.7, 128.3, 128.8, 128.8, 129.3, 129.3, 130.2, 130.6, 134.7, 134.7, 141.4, 145.5, 149.3, 168.9; ν_{max}(KBr)/cm^{-1} 1669; *m/z* (FAB) 574 (M^+ + 1) (Found: C, 81.4; H, 5.4; N, 7.2. $C_{39}H_{31}N_3O_2$ requires C, 81.65; H, 5.45; N, 7.32%).

Compound 8b. Reddish orange powder; mp 163–164 °C (from CH_2Cl_2–EtOH); δ_H (500 MHz) 3.81 (3H, s, Me), 6.19 (1H, s, CH), 6.74–6.93 (10H, m, H-5,6,7,8, NPh-3,5), 7.28 (2H, d, *J* 8.4, NPh-2,6), 7.35 (4H, d, *J* 7.3, Ph-2,6), 7.42 (2H, t, *J* 7.8, NPh-4), 7.51 (4H, dd, *J* 7.8, 7.3, NPh-3,5), 7.83 (2H, d, *J* 11.4, H-4); δ_C (125.7 MHz) 35.2, 55.2, 112.9, 113.7, 113.9, 128.4, 128.7, 129.1, 129.1, 129.4, 129.4, 130.4, 130.7, 131.6, 134.4, 141.3, 145.4, 158.0, 168.7; ν_{max}(KBr)/cm^{-1} 1685; *m/z* (FAB) 560 (M^+) (Found: C, 78.8; H, 4.9; N, 4.7. $C_{38}H_{28}N_2O_3 \cdot \frac{1}{2}H_2O$ requires C, 78.87; H, 5.23; N, 4.73%).

Compound 8c. Yellow powder; mp 189–190 °C (from CH_2Cl_2–EtOH); δ_H (500 MHz) 6.25 (1H, s, CH), 6.76 (2H, d, *J* 9.0, H-8), 6.77 (2H, dd, *J* 10.5, 8.7, H-6), 6.86 (2H, dd, *J* 10.5, 9.0, H-7), 6.91 (2H, dd, *J* 11.3, 8.7, H-5), 7.23–7.28 (1H, m, Ph-4), 7.31–7.38 (8H, m, NPh-2,6, Ph-2,3,5,6), 7.43 (2H, t, *J* 7.4, NPh-4), 7.51 (4H, dd, *J* 7.9, 7.4, NPh-3,5), 7.82 (2H, d, *J* 11.3, H-4); δ_C (125.7 MHz) 36.0, 113.0, 113.5, 126.3, 128.1, 128.4, 128.5, 128.8, 129.2, 129.4, 129.5, 130.4, 130.8, 134.5, 139.6, 141.4, 145.5, 168.8; ν_{max}(KBr)/cm^{-1} 1685; *m/z* (FAB) 530 (M^+) (Found: C, 82.2; H, 5.0; N, 5.1. $C_{37}H_{26}N_2O_2 \cdot \frac{1}{2}H_2O$ requires C, 82.35; H, 5.04; N, 5.19%).

Compound 8d. Reddish orange prisms; mp 159–160 °C (from AcOEt); δ_H (500 MHz) 6.20 (1H, s, CH), 6.78 (2H, d, *J* 9.0, H-8), 6.80 (2H, dd, *J* 10.0, 8.7, H-6), 6.89 (2H, dd, *J* 10.0, 9.0 H-7), 6.96 (2H, dd, *J* 11.4, 8.7, H-5), 7.27 (2H, d, *J* 9.0, Ph-3,5), 7.30 (2H, d, *J* 9.0, Ph-2,6), 7.35 (4H, d, *J* 7.8, NPh-2,6), 7.43 (2H, t, *J* 7.43, NPh-4), 7.52 (4H, dd, *J* 7.8, 7.3, NPh-3,5), 7.87 (2H, d, *J* 11.4, H-4); δ_C (125.7 MHz) 35.4, 112.9, 113.2, 128.5, 128.6, 128.7, 129.1, 129.4, 129.5, 129.6, 130.6, 131.1, 132.0, 134.4, 138.0, 141.6, 145.4, 168.6; ν_{max}(KBr)/cm^{-1} 1685; *m/z* (FAB) 564 (M^+) (Found: C, 77.6; H, 4.3; N, 4.9. $C_{37}H_{25}ClN_2O_2 \cdot \frac{1}{2}H_2O$ requires C, 77.41; H, 4.56; N, 4.88%).

Compound 8e. Orange powder; mp 181–182 °C (from AcOEt); δ_H (500 MHz) 6.28 (1H, s, CH), 6.83 (2H, d, *J* 9.1, H-8), 6.84 (2H, dd, *J* 9.9, 8.6, H-6), 6.93 (2H, dd, *J* 9.9, 9.1, H-7), 7.00 (2H, dd, *J* 11.5, 8.6, H-5), 7.35 (4H, d, NPh-2,6), 7.45 (2H, t, *J* 7.5, NPh-4), 7.47 (2H, d, *J* 8.4, Ph-3,5), 7.53 (4H, dd, *J* 8.2, 7.5, NPh-3,5), 7.60 (2H, d, *J* 8.4, Ph-2,6), 7.90 (2H, d, *J* 11.5, H-4); δ_C (125.7 MHz) 36.0, 110.0, 112.2, 113.5, 113.6, 119.2, 128.6, 128.9, 129.5, 129.5, 129.8, 130.9, 131.6, 132.2, 134.3, 141.8, 145.4, 145.6, 168.4; ν_{max}(KBr)/cm^{-1} 2227, 1685; *m/z* (FAB) 556 (M^++1) (Found: C, 79.4; H, 4.7; N, 6.9. $C_{38}H_{25}N_3O_2 \cdot H_2O$ requires C, 79.56; H, 4.74; N, 7.32%).

General synthetic procedure for methylium hexafluorophosphates 9a–e·PF_6^- and 10a–e·PF_6^-

To a stirred solution of heteroazulene-substituted methane derivatives **7a**–**e** and **8a**–**e** (0.25 mol) in CH_2Cl_2 (10 cm^3) was added DDQ (70 mg, 0.3 mmol) and the mixture was stirred at rt for 1 h until the reaction was completed, in each case. To the reaction mixture was added 60% aqueous HPF_6 (1 cm^3) solution and the resulting mixture was filtered. The filtrate was extracted with CH_2Cl_2, and the extract was dried over Na_2SO_4 and concentrated. The resulting residue was dissolved in CH_2Cl_2 and ether was added to the solution. The precipitated crystals were collected by filtration, and washed with ether to give the salts **9a**–**e**·PF_6^- and **10a**–**e**·PF_6^-. The results are summarized in Table l.

Compound 9a·PF_6^-. Dark brown powder; mp 211–212 °C (from CH_2Cl_2–Et_2O); δ_H (500 MHz, CD_3CN) 3.38 (6H, s, Me), 6.94 (2H, d, *J* 9.6, Ph-2,6), 7.53–7.66 (6H, m), 7.68 (2H, d, *J* 9.6, Ph-3,5), 7.77–7.82 (4H, m); δ_C (125.7 MHz, CD_3CN) 42.2, 116.3, 118.1, 123.3, 127.0, 132.1, 138.2, 139.7, 140.4, 142.2, 154.9, 156.6, 160.6, 161.9, 166.4; ν_{max}(KBr)/cm^{-1} 1749, 1268, 845; $\lambda_{max}(CH_3CN)$/nm (log (ε/mol^{-1} dm^3 cm^{-1})) 671 (4.17), 575 (4.18), 418 (sh, 3.52), 355 (3.75), 255 (4.19); *m/z* (FAB) 422 (M^+–PF_6) (Found: M^+–PF_6 422.1453. $C_{27}H_{20}F_6NO_4P$ requires M–PF_6 422.1393) (Found: C, 56.3; H, 3.7; N, 2.4. $C_{27}H_{20}F_6NO_4P \cdot \frac{1}{2}H_2O$ requires C, 56.26; H, 3.67; N, 2.43%).

Compound 9b·PF_6^-. Dark brown powder; mp 167–168 °C (from CH_3CN–Et_2O); δ_H (500 MHz, CD_3CN) 3.97 (3H, s, OMe), 7.11 (2H, d, *J* 8.8, Ph-3,5), 7.75 (2H, d, *J* 8.8, Ph-2,6), 7.77 (2H, d, *J* 10.3, H-8), 7.95 (2H, dd, *J* 10.3, 9.5, H-7), 8.01 (2H, dd, *J* 9.6, 9.5, H-6), 8.22 (2H, d, *J* 9.8, H-4), 8.27 (2H, dd, *J* 9.8, 9.6, H-5); δ_C (125.7 MHz, CD_3CN) 57.1, 109.5, 117.2, 128.4, 136.3, 137.2, 142.4, 144.9, 145.0, 154.9, 164.5, 164.8, 166.2, 167.9 (one carbon overlapping); ν_{max}(KBr)/cm^{-1} 1752, 1395, 1258, 841; $\lambda_{max}(CH_3CN)$/nm (log (ε/mol^{-1} dm^3 cm^{-1})) 621 (4.55), 537 (4.00), 381 (3.80), 281 (4.17), 248 (4.40), 224 (4.39); *m/z* (FAB) 409 (M^+–PF_6) (Found: M^+–PF_6 409.1088. $C_{26}H_{17}F_6O_5P$ requires M–PF_6 409.1076) (Found: C, 55.9; H, 3.1. $C_{26}H_{17}F_6O_5P$ requires C, 56.33; H, 3.09%).

Compound 9c·PF_6^-. Dark brown powder; mp 183–184 °C (from CH_3CN–Et_2O); δ_H (500 MHz, CD_3CN) 7.59 (2H, dd, *J* 7.9, 7.7, Ph-3,5), 7.68 (2H, d, *J* 10.2, H-8), 7.74 (2H, d, *J* 7.9, Ph-2,6), 7.82 (1H, t, *J* 7.7, Ph-4), 7.99 (2H, dd, *J* 10.2, 9.7, H-7), 8.08 (2H, t, *J* 9.7, H-6), 8.29 (2H, d, *J* 10.0, H-4), 8.35 (2H, dd, *J* 10.0, 9.7, H-5); δ_C (125.7 MHz, CD_3CN) 110.3, 129.2, 131.4,

132.8, 135.6, 138.4, 143.0, 145.2, 145.9, 154.1, 164.0, 165.4, 166.6 (one carbon overlapping); ν_{max}(KBr)/cm^{-1} 1763, 1395, 1262, 843; λ_{max}(CH_3CN)/nm (log (ε/mol^{-1} dm^3 cm^{-1})) 621 (4.18), 440 (3.47), 3.89 (3.46), 275 (3.87), 275 (3.87), 248 (4.04); *m/z* (FAB) 379 (M^+–PF_6) (Found: M^+–PF_6 379.0985. $C_{25}H_{15}F_6O_4P$ requires M–PF_6 379.0971) (Found: C, 56.7; H, 2.9; N, 1.7. $C_{25}H_{15}F_6O_4P\cdot\frac{1}{2}CH_3CN$ requires C, 57.31; H, 3.05; N, 1.29%).

Compound 9d·PF_6^-. Dark brown powder; mp 167–168 °C (from CH_3CN–Et_2O); δ_H (500 MHz, CD_3CN) 7.61 (2H, d, *J* 8.7, Ph-3,5), 7.72 (2H, d, *J* 8.7, Ph-2,6), 7.76 (2H, d, *J* 10.8, H-8), 8.05 (2H, dd, *J* 10.8, 9.6, H-7), 8.11 (2H, dd, *J* 10.0, 9.6, H-6), 8.30 (2H, d, *J* 10.0, H-4), 8.38 (2H, t, 10.0, H-5); δ_C (125.7 MHz, CD_3CN) 110.0, 129.3, 131.5, 134.4, 134.6, 138.5, 141.6, 143.1, 145.4, 146.0, 153.6, 163.9, 164.7, 165.4; ν_{max}(KBr)/cm^{-1} 1763, 1395, 1260, 844; λ_{max}(CH_3CN)/nm (log (ε/mol^{-1} dm^3 cm^{-1})) 621 (4.32), 456 (sh, 3.76), 398 (3.95), 278 (sh, 4.12), 250 (4.35), 220 (4.39); *m/z* (FAB) 413 (M^+–PF_6) (Found: M^+–PF_6 413.0569. $C_{25}H_{14}ClF_6O_4P$ requires M–PF_6 413.0581) (Found: C, 54.7; H, 2.5; N, 0.6. $C_{25}H_{14}ClF_6O_4P\cdot\frac{1}{3}CH_3CN$ requires C, 54.17; H, 2.62; N, 0.81%).

Compound 9e·PF_6^-. Dark brown powder; mp 173–174 °C (from CH_2Cl_2–Et_2O); δ_H (500 MHz, CD_3CN) 7.69 (2H, d, *J* 10.5, H-8), 7.86 (2H, d, *J* 8.6, Ph-3,5), 7.92 (2H, d, *J* 8.6, Ph-2,6), 8.09 (2H, dd, *J* 10.5, 9.5, H-7), 8.16 (2H, dd, *J* 9.8, 9.5, H-6), 8.35 (2H, d, *J* 10.2, H-4), 8.43 (2H, dd, *J* 10.2, 9.8, H-5); δ_C (125.7 MHz, CD_3CN) 110.2, 117.4, 119.1, 129.7, 133.2, 134.8, 139.2, 140.5, 143.5, 145.7, 146.6, 153.0, 163.8, 165.8 (one carbon overlapping); ν_{max}(KBr)/cm^{-1} 2227, 1735, 1266, 839; λ_{max}(CH_3CN)/nm (log (ε/mol^{-1} dm^3 cm^{-1})) 621 (3.62), 391 (3.98), 262 (4.18), 225 (4.28); *m/z* (FAB) 404 (M^+–PF_6) (Found: M^+–PF_6 404.0943. $C_{26}H_{14}F_6NO_4P$ requires M–PF_6 404.0923) (Found: C, 51.5; H, 2.4; N, 2.3. $C_{26}H_{14}F_6NO_4P\cdot CH_2Cl_2$ requires C, 51.13; H, 2.54; N, 2.55%).

Compound 10a·PF_6^-. Dark brown powder; mp 212–214 °C (from CH_2Cl_2–Et_2O); δ_H (500 MHz, CD_3CN) 3.30 (3H, s, NMe), 6.91 (2H, d, *J* 8.8, Ph-3,5), 7.42–7.45 (6H, m), 7.50 (2H, dd, *J* 9.8, 9.3), 7.54 (2H, d, *J* 10.3, H-4), 7.59 (2H, t, *J* 7.3, NPh-4), 7.63–7.70 (8H, m), 7.75 (2H, d, *J* 8.8, Ph-2,6); δ_C (125.7 MHz, CD_3CN) 41.1, 114.3, 120.3, 125.1, 128.3, 129.6, 130.0, 131.1, 132.1, 133.3, 134.9, 135.7, 138.0, 138.5, 148.8, 150.2, 157.6, 159.6, 174.1; ν_{max}(KBr)/cm^{-1} 1685, 843; λ_{max}(CH_3CN)/nm (log (ε/mol^{-1} dm^3 cm^{-1})) 677 (4.67), 614 (sh, 4.58), 411 (3.93), 298 (4.51), 262 (4.53); *m/z* (FAB) 572 (M^+–PF_6) (Found: M^+–PF_6 572.2354. $C_{39}H_{30}F_6N_3O_2P$ requires M–PF_6 572.2326) (Found: C, 65.5; H, 4.1; N, 5.9. $C_{39}H_{30}F_6N_3O_2P$ requires C, 65.27; H, 4.21; N, 5.86%).

Compound 10b·PF_6^-. Dark brown powder; mp 272–273 °C (from CH_2Cl_2–Et_2O); δ_H (500 MHz, CD_3CN) 3.95 (3H, s, OMe), 7.10 (2H, d, *J* 9.0, Ph-3,5), 7.46 (4H, d, *J* 6.0, NPh-2,6), 7.61 (2H, t, *J* 7.3, NPh-4), 7.65–7.68 (6H, m), 7.71–7.73 (4H, m), 7.76 (2H, d, *J* 9.0, Ph-2,6), 7.87–7.94 (4H, m); δ_C (125.7 MHz, CD_3CN) 56.6, 114.8, 116.4, 124.2, 129.0, 130.2, 130.7, 130.9, 134.3, 135.7, 136.2, 138.5, 140.9, 142.4, 149.6, 154.0, 163.3, 165.4, 166.4; ν_{max}(KBr)/cm^{-1} 1696, 838; λ_{max}(CH_3CN)/nm (log (ε/mol^{-1} dm^3 cm^{-1})) 652 (4.61), 534 (4.05), 419 (3.79), 305 (4.47); *m/z* (FAB) 559 (M^+–PF_6) (Found: M^+–PF_6 559.2050. $C_{38}H_{27}F_6N_2O_3P$ requires M–PF_6 559.2023) (Found: C, 63.6; H, 3.6; N, 4.2. $C_{38}H_{27}F_6N_2O_3P\cdot\frac{1}{2}H_2O$ requires C, 63.96; H, 3.95; N, 3.93%).

Compound 10c·PF_6^-. Dark brown powder; mp 258–259 °C (from CH_3CN–Et_2O); δ_H (500 MHz, CD_3CN) 7.47 (4H, d, *J* 6.8, NPh-2,6), 7.57 (2H, dd, *J* 8.5, 7.3, Ph-3,5), 7.62 (2H, t, *J* 7.3, NPh-4), 7.67 (4H, dd, *J* 7.3, 6.8, NPh-3,5), 7.70–7.81 (11H, m), 7.98 (2H, t, *J* 10.0, H-5); δ_C (125.7 MHz, CD_3CN) 115.7, 125.0, 129.2, 130.9, 131.0, 131.2, 133.2, 134.4, 134.4, 136.8, 138.5, 139.2, 141.4, 143.3, 149.2, 154.8, 163.5, 165.3; ν_{max}(KBr)/cm^{-1} 1696, 840; λ_{max}(CH_3CN)/nm (log (ε/mol^{-1} dm^3 cm^{-1})) 652 (4.93), 478 (3.99), 402 (sh, 4.11), 357 (sh, 432), 303 (4.63); *m/z* (FAB) 529 (M^+–PF_6) (Found: M^+–PF_6 529.1943. $C_{37}H_{25}F_6N_2O_2P$ requires M–PF_6 529.1918) (Found: C, 65.1; H, 3.7; N, 5.7. $C_{37}H_{25}F_6N_2O_2P\cdot CH_3CN$ requires C, 65.5; H, 3.94; N, 5.87%).

Compound 10d·PF_6^-. Dark brown powder; mp 270–271 °C (from CH_2Cl_2–Et_2O); δ_H (500 MHz, CD_3CN) 7.47 (4H, d, *J* 6.9, NPh-2,6), 7.57 (2H, d, *J* 8.7, NPh-3,5), 7.62 (2H, t, *J* 7.3, NPh-4), 7.67 (4H, dd, *J* 7.3, 6.9, NPh-3,5), 7.72 (2H, d, *J* 10.2, H-8), 7.75 (2H, d, *J* 8.7, Ph-2,6), 7.78–7.82 (4H, m), 7.86–7.89 (2H, m), 7.97–8.03 (2H, m); δ_C (125.7 MHz, CD_3CN) 115.3, 125.2, 129.2, 131.0, 131.0, 131.2, 134.3, 134.9, 137.0, 139.3, 140.3, 141.7, 143.5, 148.9, 154.9, 161.6, 165.3 (one carbon overlapping); ν_{max}(KBr)/cm^{-1} 1696, 841; λ_{max}(CH_3CN)/nm (log (ε/mol^{-1} dm^3 cm^{-1})) 652 (4.97), 487 (3.94), 404 (4.05), 358 (sh, 4.21), 302 (4.54); *m/z* (FAB) 563 (M^+–PF_6) (Found: M^+–PF_6 563.1566. $C_{37}H_{24}ClF_6N_2O_2P$ requires M–PF_6 563.1528) (Found: C, 61.9; H, 3.2; N, 3.8. $C_{37}H_{24}ClF_6N_2O_2P\cdot\frac{1}{3}H_2O$ requires C, 62.15; H, 3.48; N, 3.92%).

Compound 10e·PF_6^-. Dark brown powder; mp 262–264 °C (from CH_2Cl_2–Et_2O); δ_H (500 MHz, CD_3CN) 7.47 (4H, d, *J* 7.6, NPh-2,6), 7.62 (2H, t, *J* 7.3, NPh-4), 7.67 (4H, dd, *J* 7.6, 7.3, NPh-3,5), 7.76 (2H, d, *J* 10.6, H-8), 7.81–7.90 (10H, m), 8.02–8.07 (2H, m); δ_C (125.7 MHz, CD_3CN) 115.2, 116.3, 119.3, 125.5, 129.1, 131.1, 131.2, 133.6, 134.2, 134.2, 137.5, 139.6, 141.9, 142.9, 144.0, 148.2, 155.3, 160.3, 165.2; ν_{max}(KBr)/cm^{-1} 2227, 1701, 838; λ_{max}(CH_3CN)/nm (log (ε/mol^{-1} dm^3 cm^{-1})) 652 (4.52), 459 (sh, 3.65), 402 (3.83), 359 (sh, 4.00), 315 (4.33), 245 (4.54); *m/z* (FAB) 554 (M^+–PF_6) (Found: M^+–PF_6 554.1873. $C_{38}H_{24}F_6N_3O_2P$ requires M–PF_6 554.1870) (Found: C, 64.5; H, 3.3; N, 6.0. $C_{38}H_{24}F_6N_3O_2P$ requires C, 65.24; H, 3.46; N, 6.01%).

Determination of the pK_{R^+} value of methyl cations 9a–e and 10a–e

Buffer solutions of slightly different acidities were prepared by mixing aqueous solutions of KH_2PO_4 (0.1 M) and NaOH (0.1 M) (for pH 6.0–8.0), $Na_2B_4O_7$ (0.025 M) and HCl (0.1 M) (for pH 8.2–9.0), $Na_2B_4O_7$ (0.025 M) and NaOH (0.1 M) (for pH 9.2–10.8), Na_2HPO_4 (0.05 M) and NaOH (0.1 M) (for pH 11.0–12.0), and KCl (0.2 M) and NaOH (0.1 M) (for pH 12.0–14.0) in various portions. For the preparation of sample solutions, 1 cm^3 portions of the stock solution, prepared by dissolving 3–5 mg of the cation **9a**–**e**·PF_6^- and **10a**–**e**·PF_6^- in MeCN (20 cm^3), were diluted to 10 cm^3 with the buffer solution (8 cm^3) and MeCN (1 cm^3). The UV–vis spectrum was recorded for each cation **9a**–**e**·PF_6^- and **10a**–**e**·PF_6^- in 10 different buffer solutions. Immediately after recording the spectrum, the pH of each solution was determined on a pH meter calibrated with standard buffers. The observed absorbance at the specific absorption wavelengths (664 nm for **9a**; 604 nm for **9b**; 606 nm for **9c**; 608 nm for **9d**; 606 nm for **9e**; 665 nm for **10a**; 632 nm for **10b**; 634 nm for **10c**; 634 nm for **10d**; 635 nm for **10e**) of each cation **9a**–**e**·PF_6^- and **10a**–**e**·PF_6^- was plotted against pH to give a classical titration curve, whose midpoint was taken as the pK_{R^+} value.

Cyclic voltammetry of methyl cations 9a–e and 10a–e

The reduction potentials of **9a**–**e** and **10a**–**e** were determined by means of a CV-27 voltammetry controller (BAS Co). A three-electrode cell was used, consisting of Pt working and counter electrodes and a reference Ag/$AgNO_3$ electrode. Nitrogen was bubbled through an acetonitrile solution (4 cm^3) of each compound (0.5 mmol dm^{-3}) and Bu_4NClO_4 (0.1 mol dm^{-3}) to

deaerate it. The measurements were made at a scan rate of 0.1 V s^{-1} and the voltammograms were recorded on a WX-1000-UM-019 (Graphtec Co) X-Y recorder. Immediately after the measurements, ferrocene (0.1 mmol) ($E_{1/2}$ = +0.083) was added as the internal standard, and the observed peak potentials were corrected with reference to this standard. The compounds exhibited reversible reduction–oxidation waves; the results are summarized in Table 2.

Acknowledgements

Financial support from Waseda University Grants for Special Research Projects is gratefully acknowledged. The authors also thank the Materials Characterization Central Laboratory, Waseda University, for technical assistance with the special data and elemental analyses.

References

1 S. Ito, N. Morita and T. Asao, *Tetrahedron Lett.*, 1991, **32**, 773. Synthesis of the tris(4,6,8-trimethylazulen-1-yl)methyl cation is previously reported, K. Hafner, H. Pelster and J. Schneider, *Liebigs Ann. Chem.*, 1961, **650**, 62.
2 S. Ito, N. Morita and T. Asao, *Tetrahedron Lett.*, 1994, **35**, 751.
3 S. Ito, N. Morita and T. Asao, *Tetrahedron Lett.*, 1994, **35**, 3723.
4 S. Ito, N. Morita and T. Asao, *Bull. Chem. Soc. Jpn.*, 1995, **68**, 1409.
5 S. Ito, N. Morita and T. Asao, *Bull. Chem. Soc. Jpn.*, 1995, **68**, 2011; S. Ito, N. Morita and T. Asao, *Bull. Chem. Soc. Jpn.*, 1995, **68**, 2639.
6 S. Ito, S. Kikuchi, N. Morita and T. Asao, *Bull. Chem. Soc. Jpn.*, 1999, **72**, 839.
7 S. Ito, S. Kikuchi, N. Morita and T. Asao, *J. Org. Chem.*, 1999, **64**, 5815.
8 S. Ito, M. Fujita, N. Morita and T. Asao, *Chem. Lett.*, 1995, 475; S. Ito, M. Fujita, N. Morita and T. Asao, *Bull, Chem. Soc. Jpn.*, 1995, **68**, 3611.
9 S. Ito, H. Kobayashi, S. Kikuchi, N. Morita and T. Asao, *Bull. Chem. Soc. Jpn.*, 1996, **69**, 3225.
10 S. Ito, S. Kikuchi, H. Kobayashi, N. Morita and T. Asao, *J. Org. Chem.*, 1997, **62**, 2423.
11 S. Seto, *Sci. Rep. Tohoku Univ.*, *Ser. 1*, 1953, **37**, 367.
12 M. Nitta and S. Naya, *J. Chem. Res.* (*S*), 1998, 522; M. Nitta and S. Naya, *J. Chem. Res.* (*M*), 1998, 2263.
13 R. W. Alder and C. Wilshire, *J. Chem. Soc.*, *Perkin Trans. 2*, 1975, 1464; T. Nozoe, T. Toda, T. Asao and A. Yamanouchi, *Bull. Chem. Soc. Jpn.*, 1968, **41**, 2935.
14 N. Abe and T. Takehiro, *Chem. Lett.*, 1987, 1727; N. Abe and T. Takehiro, *Bull. Chem. Soc. Jpn.*, 1988, **61**, 1225.
15 S. Naya and M. Nitta, *J. Chem. Soc.*, *Perkin. Trans. 1*, 2000, 2777.
16 E. M. Arnett and R. D. Bushick, *J. Am. Chem. Soc.*, 1964, **86**, 1564.
17 M. J. S. Dewar, E. G. Zoebisch, E. F. Healy and J. J. P. Stewart, *J. Am. Chem. Soc.*, 1985, **107**, 3902; M. J. S. Dewar and E. G. Zoebisch, *THEOCHEM*, 1988, **180**, 1.
18 C. D. Ritchie, W. F. Sager and E. S. Lewis, *J. Am. Chem. Soc.*, 1962, **84**, 2349.
19 S. Lovell, B. J. Marquardt and B. Kahr, *J. Chem. Soc.*, *Perkin. Trans. 2*, 1999, 2241.
20 H. H. Freedman, in *Carbonium Ions*, eds. G. A. Olah and P. v. R. Schleyer, Wiley-Interscience, New York, 1973.
21 H. G. Viehe, R. Merényi, L. Stella and Z. Janousek, *Angew. Chem.*, *Int. Ed. Engl.*, 1979, **18**, 917 and references cited therein.
22 K. Okamoto, K. Takeuchi, K. Komatsu, Y. Kubota, R. Ohara, M. Arima, K. Takahashi, Y. Waki and S. Shirai, *Tetrahedron*, 1983, **39**, 4011 and references cited therein.
23 C. Hansch, A. Leo and R. W. Taft, *Chem. Rev.*, 1991, **91**, 165.
24 J. Griffiths and K. J. Pender, *Dyes Pigm.*, 1981, **2**, 37.